Chapter 8

Waveguides and Resonators

The objective of resonators is to *confine* electromagnetic energy. On the other hand, the purpose of waveguides is to *guide* electromagnetic energy. In both cases, the desired functionality is achieved through material boundaries.

8.1 Resonators

Let us consider a rectangular box with sides L_x, L_y, and L_z, as shown in Fig. 8.1. The interior of the box is filled with a linear and isotropic material characterized by ε and μ. The walls of the box are perfectly reflecting, that is, the fields are not able to penetrate into the walls. Furthermore, there are no sources present, which implies that we're looking for homogeneous solutions of the wave equation, that is, solutions of the Helmholtz equation (3.15).

To solve the Helmholtz equation for the x component of the complex electric field vector $\mathbf{E}$ we write

$$E_x(x,y,z) = E_0^{(x)}\, X(x)\, Y(y)\, Z(z)\;, \tag{8.1}$$

which is referred to as *separation of variables*. X, Y, and Z are dimensionless functions and $E_0^{(x)}$ is a constant field amplitude. Inserting into $[\nabla^2 + k^2]E_x = 0$ yields

$$\frac{1}{X}\frac{\partial^2 X}{\partial x^2} + \frac{1}{Y}\frac{\partial^2 Y}{\partial y^2} + \frac{1}{Z}\frac{\partial^2 Z}{\partial z^2} + k^2 = 0\;. \tag{8.2}$$

In order for this equation to hold for any x, y, and z we have to require that each of the terms is constant. We set these constants to be $-k_x^2$, $-k_y^2$ and $-k_z^2$, which implies

$$k_x^2 + k_y^2 + k_z^2 \;=\; k^2 \;=\frac{\omega^2}{c^2} n^2(\omega)\;. \tag{8.3}$$

We obtain three separate equations for X, Y, and Z

$$\begin{aligned} \partial^2 X \,/\, \partial x^2 \;+\; k_x^2 X \;&=\; 0 \\ \partial^2 Y \,/\, \partial y^2 \;+\; k_y^2 Y \;&=\; 0 \\ \partial^2 Z \,/\, \partial z^2 \;+\; k_z^2 Z \;&=\; 0\,, \end{aligned} \tag{8.4}$$

with the solutions $\exp[\pm i k_x x]$, $\exp[\pm i k_y y]$, and $\exp[\pm i k_z z]$. Thus, the solutions for E_x become

$$E_x(x,y,z) = E_0^{(x)} \left[c_{1,x}\,\mathrm{e}^{-ik_x x} + c_{2,x}\,\mathrm{e}^{ik_x x}\right]\left[c_{3,x}\,\mathrm{e}^{-ik_y y} + c_{4,x}\,\mathrm{e}^{ik_y y}\right]\left[c_{5,x}\,\mathrm{e}^{-ik_z z} + c_{6,x}\,\mathrm{e}^{ik_z z}\right]. \tag{8.5}$$

Electric fields cannot penetrate into a perfect conductor. Therefore, the boundary condition (4.13) implies $E_x(x=0) = E_x(x=L_x) = 0$, which turns Eq. (8.5) into

$$E_x(x,y,z) \;=\; E_0^{(x)}\;\sin[n\,\pi\,x/L_x]\left[c_{3,x}\,\mathrm{e}^{-ik_y y} + c_{4,x}\,\mathrm{e}^{ik_y y}\right]\left[c_{5,x}\,\mathrm{e}^{-ik_z z} + c_{6,x}\,\mathrm{e}^{ik_z z}\right]\,, \tag{8.6}$$

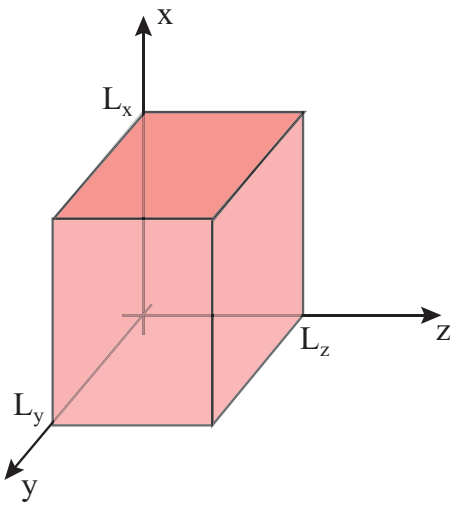

Figure 8.1: A resonator with perfectly reflecting walls and side lengths L_x, L_y, and L_z .

with n being an integer. Similar solutions are found for E_y and E_z, namely,

$$E_y(x,y,z) = E_0^{(y)} \left[c_{1,y}\, e^{-ik_x x} + c_{2,y}\, e^{ik_x x}\right] \sin[m\,\pi\, y/L_y] \left[c_{5,y}\, e^{-ik_z z} + c_{6,y}\, e^{ik_z z}\right] \quad (8.7)$$

$$E_z(x,y,z) = E_0^{(z)} \left[c_{1,z}\, e^{-ik_x x} + c_{2,z}\, e^{ik_x x}\right] \left[c_{3,z}\, e^{-ik_y y} + c_{4,z}\, e^{ik_y y}\right] \sin[l\,\pi\, z/L_z]. \quad (8.8)$$

Because $\nabla \cdot \mathbf{E} = 0$ for any x, y, and z we find

$$\begin{aligned} E_x(x,y,z) &= E_0^{(x)} \sin[n\,\pi\, x/L_x] \sin[m\,\pi\, y/L_y] \sin[l\,\pi\, z/L_z] \\ E_y(x,y,z) &= E_0^{(y)} \sin[n\,\pi\, x/L_x] \sin[m\,\pi\, y/L_y] \sin[l\,\pi\, z/L_z] \\ E_z(x,y,z) &= E_0^{(z)} \sin[n\,\pi\, x/L_x] \sin[m\,\pi\, y/L_y] \sin[l\,\pi\, z/L_z]\,, \end{aligned} \quad (8.9)$$

and

$$\frac{n}{L_x} E_0^{(x)} + \frac{m}{L_y} E_0^{(y)} + \frac{l}{L_z} E_0^{(z)} = 0 \quad (8.10)$$

Using Eq. (8.3) we find the dispersion relation or mode structure of the resonator

$$\pi^2 \left[\frac{n^2}{L_x^2} + \frac{m^2}{L_y^2} + \frac{l^2}{L_z^2}\right] = \frac{\omega_{nml}^2}{c^2}\, n^2(\omega_{nml}) \qquad n,m,l \in \{0,1,2,3,..\} \quad (8.11)$$

Thus, we find that the resonator supports only discrete frequencies ω_{nml}, each associated with a mode (n,m,l) of the resonator. Note that n is used both for the index of refraction and for the mode number in x.

8.1.1 The Density of States

Let us now consider a resonator with equal sides, that is, $L = L_x + L_y + L_z$. In this case,

$$n^2 + m^2 + l^2 = \left[\frac{\omega_{nml}\, L\, n(\omega_{nml})}{\pi\, c}\right]^2 . \quad (8.12)$$

If n, m, and l were real numbers, then this equation defines a sphere of radius $r_0 = [omega_{nml}\, L\, n(\omega_{nml})/(\pi\, c)]$. Indeed, for large numbers we can approximate these numbers by real numbers. Let us now consider a specific mode given by $[n,m,l]$ and with angular frequency $\omega = \omega_{nml}$ and count the number of modes N with frequencies smaller than ω. According to Eq. (8.12) this corresponds to the

interior of a sphere with radius r_0, and because n, m, and l are positive numbers we have to count only $1/8$-th of the sphere. Thus,

$$N(\omega) = \frac{1}{8}\left[\frac{4\pi}{3} r_0^3\right] \; 2 \; . \tag{8.13}$$

The '2' at the end has been added because for each $[n, m, l]$ there are two solutions with different polarizations. This follows from Eq. (8.10). Inserting the expression for r_0 we find

$$N(\omega) = V \, \frac{\omega^3 \, n^3(\omega)}{3\pi^2 \, c^3} \; , \tag{8.14}$$

where V is the volume of the resonator. The number of different resonator modes in the frequency interval $[\omega \; .. \; \omega + \Delta\omega]$ becomes

$$\frac{d \, N(\omega)}{d\omega} \, \Delta\omega \;\; = \;\; V \, \frac{\omega^2 \, n^3(\omega)}{\pi^2 \, c^3} \, \Delta\omega \; , \tag{8.15}$$

which states that there a many more modes for high frequencies ω. We now define the number of modes $\rho(\omega)$ per unit volume V and unit frequency $\Delta\omega$. We obtain

$$\rho(\omega) \;\; = \;\; \frac{\omega^2 \, n^3(\omega)}{\pi^2 \, c^3} \tag{8.16}$$

which is generally referred to as the *density of states* (DOS). The number of modes N in the volume V and in the frequency range $[\omega_1 \; .. \; \omega_2]$ is then calculated as

$$N(\omega) \;\; = \;\; \int_V \int_{\omega_1}^{\omega_2} \rho(\omega) \, d\omega \, dV \; . \tag{8.17}$$

The density of states is of importance in blackbody radiation and is an important concept to describe how efficient radiation interacts with matter. For example, the power $\bar{P}$ emitted by a dipole (c.f. Eq 6.46) can be expressed in terms of the density of states as

$$\bar{P} \;\; = \;\; \frac{\pi \, \omega^2}{12 \, \varepsilon_0 \, \varepsilon} \; |\mathbf{p}| \; \rho(\omega) \tag{8.18}$$

As we discussed in Section 6.4, the amount of radiation released by a dipole depends on the environment, and this dependence can be accounted for by the density of states rho. In other words, ρ depends on the specific environment and takes on a value of $\omega^2 \, / \, \pi^2 c^3$ in empty space (vacuum). Any objects placed into the empty space will influence ρ and the ability of a dipole source to radiate.

The resonator that we have analyzed possesses discrete frequencies ω_{mnl}. In reality, any resonator has losses, for example due to the absorption of electromagnetic energy at the boundaries or due to radiation. As a consequence, the discrete frequencies broaden and assume a finite line width $\Delta\omega = 2\gamma$. The quality factor, or Q-factor of a line is defined as $Q = \omega/(2\gamma)$. It is a measure for how long electromagnetic energy can be stored in a resonator. The line shape of a mode is generally a Lorentzian (see Section 6.7). The electric field in the cavity is therefore an exponentially damped oscillation of the form

$$\mathbf{E}(\mathbf{r},t) \;=\; \mathrm{Re}\left\{\mathbf{E}_0(\mathbf{r})\,\exp\left[(\mathrm{i}\omega_0 - \frac{\omega_0}{2\,Q})\,t\right]\right\}\;, \tag{8.19}$$

where ω_0 represents one of the resonance frequencies ω_{mnl}. The spectrum of the stored energy density becomes

$$W_\omega(\omega) \;=\; \frac{\omega_0^2}{4Q^2}\,\frac{W_\omega(\omega_0)}{(\omega-\omega_0)^2 \;+\; (\omega_0\,/\,2Q)^2}\;. \tag{8.20}$$

8.1.2 Cavity Perturbation

A sharp resonance is a key requirement for ultrasensitive detection in various applications. For example, watches and clocks use high-Q quartz crystals to measure time, some biosensing schemes make use of oscillating cantilevers to detect adsorption of molecules, and atomic clocks use atomic resonances as frequency standards. A perturbation of the resonator (cavity), for example due to particle adsorption or a change of the index of refraction, leads to a shift of the resonance frequency, which can be measured and used as a control signal for sensing.

To establish an understanding of cavity perturbation we consider the system depicted in Fig. 8.2. A leaky cavity and its environment are characterized by a spatially varying permittivity $\varepsilon(\mathbf{r})$ and permeability $\mu(\mathbf{r})$. In the absence of any perturbation the system assumes a resonance at frequency ω_0 and the the fields are described by

$$\nabla\times\mathbf{E}_0 \;=\; i\omega_0\mu_0\mu(\mathbf{r})\mathbf{H}_0\,,\quad \nabla\times\mathbf{H}_0 \;=\; -i\omega_0\varepsilon_0\varepsilon(\mathbf{r})\mathbf{E}_0\,, \tag{8.21}$$

with $\mathbf{E}_0(\mathbf{r},\omega_0)$ and $\mathbf{H}_0(\mathbf{r},\omega_0)$ denoting the unperturbed complex field amplitudes. A particle with material parameters $\Delta\varepsilon(\mathbf{r})$, $\Delta\mu(\mathbf{r})$ constitutes a perturbation and gives

rise to a new resonance frequency ω. Maxwell's curl equations for the perturbed system read as

$$\nabla \times \mathbf{E} \;=\; i\omega\mu_0 \left[\mu(\mathbf{r})\mathbf{H} + \Delta\mu(\mathbf{r})\mathbf{H}\right] \tag{8.22}$$

$$\nabla \times \mathbf{H} \;=\; -i\omega\varepsilon_0 \left[\varepsilon(\mathbf{r})\mathbf{E} + \Delta\varepsilon(\mathbf{r})\mathbf{E}\right] . \tag{8.23}$$

Notice that both $\Delta\varepsilon$ and $\Delta\mu$ are zero outside of the volume occupied by the perturbation. Using $\nabla \cdot (\mathbf{A} \times \mathbf{B}) = (\nabla \times \mathbf{A}) \cdot \mathbf{B} - (\nabla \times \mathbf{B}) \cdot \mathbf{A}$ we find

$$\begin{aligned} \nabla \cdot \left[\mathbf{E}_0^* \times \mathbf{H} - \mathbf{H}_0^* \times \mathbf{E}\right] = {} & i(\omega - \omega_0) \left[\varepsilon_0\varepsilon(\mathbf{r})\mathbf{E}_0^* \cdot \mathbf{E} \;+\; \mu_0\mu(\mathbf{r})\mathbf{H}_0^* \cdot \mathbf{H}\right] \\ & +\; i\omega \left[\mathbf{E}_0^*\varepsilon_0\Delta\varepsilon(\mathbf{r})\mathbf{E} \;+\; \mathbf{H}_0^*\mu_0\Delta\mu(\mathbf{r})\mathbf{H}\right] . \end{aligned} \tag{8.24}$$

We now consider a fictitious spherical surface ∂V at very large distance from the cavity and integrate Eq. (8.24) over the enclosed volume V (c.f. Fig. 8.2). Using Gauss' theorem, the left hand side of Eq. (8.24) becomes

$$\int_{\partial V} \left[\mathbf{H} \cdot (\mathbf{n} \times \mathbf{E}_0^*) \;+\; \mathbf{H}_0^* \cdot (\mathbf{n} \times \mathbf{E})\right] da \;=\; 0 \tag{8.25}$$

where $\mathbf{n}$ is a unit vector normal to the surface ∂V. The above expression vanishes because of the transversality of the field, i.e. $(\mathbf{n} \times \mathbf{E}_0^*) = (\mathbf{n} \times \mathbf{E}) = 0$ on the surface

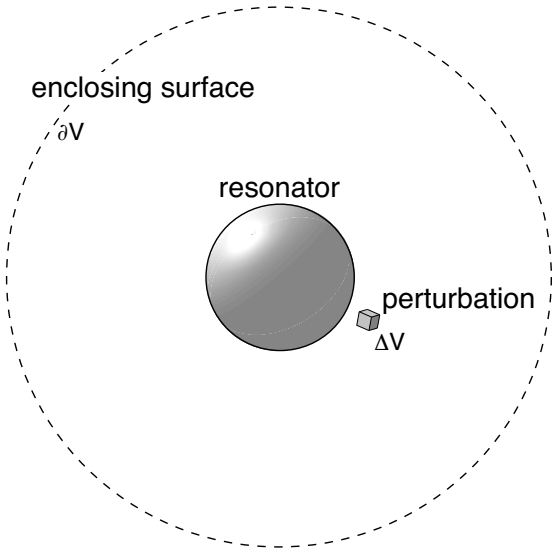

Figure 8.2: A resonator with resonance frequency ω_0 interacts with an external perturbation giving rise to a new resonance frequency ω. The calculation makes use of a fictitious spherical surface at infinity.

of the spherical surface. We thus arrive at the equation

$$\frac{\omega-\omega_0}{\omega} \;=\; -\frac{\int_V[\mathbf{E}_0^*\varepsilon_0\Delta\varepsilon(\mathbf{r})\mathbf{E} \;+\; \mathbf{H}_0^*\mu_0\Delta\mu(\mathbf{r})\mathbf{H}]\,dV}{\int_V\left[\varepsilon_0\varepsilon(\mathbf{r})\mathbf{E}_0^*\cdot\mathbf{E} \;+\; \mu_0\,\mu(\mathbf{r})\mathbf{H}_0^*\cdot\mathbf{H}\right]\,dV}\,, \tag{8.26}$$

which is known as the Bethe-Schwinger cavity perturbation formula. Eq. (8.26) is an exact formula, but because $\mathbf{E}$ and $\mathbf{H}$ are not known the equation cannot be used in its form. Notice that because $\Delta\varepsilon$ and $\Delta\mu$ are zero outside of the volume occupied by the perturbation the integral in the nominator runs only over the volume of the perturbation ΔV. For situations where there are no radiation losses and all the energy is contained inside the boundaries of a resonator the surface ∂V can be chosen to coincide with the boundaries.

We assume that the perturbation has a small effect on the cavity. Therefore we write as a first-order approximation $\mathbf{E}=\mathbf{E}_0$ and $\mathbf{H}=\mathbf{H}_0$. After performing these substitutions in Eq. (8.26) we find

$$\frac{\omega-\omega_0}{\omega} \;\approx\; -\frac{\int_{\Delta V}[\mathbf{E}_0^*\varepsilon_0\Delta\varepsilon(\mathbf{r})\mathbf{E}_0 \;+\; \mathbf{H}_0^*\mu_0\Delta\mu(\mathbf{r})\mathbf{H}_0]\,dV}{\int_V\left[\varepsilon_0\varepsilon(\mathbf{r})\mathbf{E}_0^*\cdot\mathbf{E}_0 \;+\; \mu_0\,\mu(\mathbf{r})\mathbf{H}_0^*\cdot\mathbf{H_0}\right]\,dV} \tag{8.27}$$

For a high-Q resonator the radiation losses are small and the integration volume V can be taken over the boundaries of the resonator. To evaluate Eq. (8.27) we first must solve for the fields $\mathbf{E}_0(\mathbf{r}),\mathbf{H}_0(\mathbf{r})$ of the unperturbed cavity. Interestingly, for a weakly-dispersive medium the denominator of Eq. (8.27) denotes the total energy of the unperturbed cavity (W_0) whereas the nominator accounts for the energy introduced by the perturbation (ΔW). Hence, $(\omega-\omega_0)/\omega = -\Delta W/W_0$. An increase of energy by ΔW causes the resonance frequency to *red-shift* to $\omega=\omega_0\,[W_0/(W_0+\Delta W)]$. A *blue-shift* is possible by perturbing the cavity volume, i.e. by removing ΔW from the cavity.

As an example let us consider a planar cavity with perfectly reflecting end faces of area A and separated by a distance L. The fundamental mode $\lambda=2L$ has a resonance frequency $\omega_0=\pi c/L$, and the electric and magnetic fields inside the cavity are calculated to be $E_0\sin[\pi z/L]$ and $-i\sqrt{\varepsilon_0/\mu_0}E_0\cos[\pi z/L]$, respectively. The coordinate z is perpendicular to the surfaces of the end faces. The denominator of Eq. (8.27) is easily determined to be $V\,\varepsilon_0\,E_0^2$, where $V=LA$. We place a spherical nanoparticle with dielectric constant $_\Delta\varepsilon$ and volume $_\Delta V$ in the center of

the cavity and assume that the field is homogeneous across the dimensions of the particle. The nominator of Eq. (8.27) is calculated to be $\Delta V\, \Delta\varepsilon\, \varepsilon_0\, E_0^2$ and the frequency shift is determined to be $(\omega - \omega_0)/\omega = -\Delta\varepsilon\, \Delta V/V$. A better approximation retains the perturbed fields $\mathbf{E}$ and $\mathbf{H}$ in the nominator of Eq. (8.26). Making use of the quasi-static solution for a small spherical particle we write $\mathbf{E} = 3\mathbf{E}_0/(2 + \Delta\varepsilon)$ and obtain a frequency shift of $(\omega - \omega_0)/\omega = -[3\Delta\varepsilon/(2 + \Delta\varepsilon)]\, \Delta V/V$. In both cases the resonance shift scales with the ratio of resonator and perturbation volumes.

8.2 Waveguides

Waveguides are used to carry electromagnetic energy from location A to location B. They exist in form of wires, coaxial cables, parallel plates, or optical fibers. In general, the transmission of radiation through free-space is subject to diffraction, which results in spreading out of energy. Waveguides avoid this problem at the expense of material structures that have to connect the locations A and B.

The simplest waveguide system is the two-wire transmission line. It can be formulated in terms of distributed circuit elements, such as capacitances C and inductances L. One can derive a one-dimensional wave equation for the current and the voltage carried along the transmission line. The speed of propagation is given by $c = 1/\sqrt{L\,C}$. Detailed discussions of transmission lines can be found in many textbooks and we won't derive or analyze it here. Instead, we will concentrate on parallel-plate waveguide and on hollow metal waveguides and then make a transition to all-dielectric waveguides used in fiber-optic communication.

8.2.1 Parallel-Plate Waveguides

The parallel-plate waveguide that we consider here is illustrated in Fig. 8.3. It consists of a medium characterized by the index of refraction $n(\omega)$ sandwiched between two ideally conducting plates. We will align our coordinate system such that the wave propagates in direction of the z axis. As we shall see, one distinguishes between two different solutions: 1) Waves that have no electric field in propagation

direction z (TE modes), and 2) waves that have no magnetic field in propagation direction z (TM modes).

TE Modes

For TE modes the electric field is parallel to the surface of the plates. As an ansatz we choose a plane wave propagating at an angle θ towards the bottom plate

$$\mathbf{E}_1(x,y,z) \;=\; E_0\,\mathbf{n}_y\,\exp[-ikx\cos\theta + ikz\sin\theta]\;, \tag{8.28}$$

with $k = n(\omega)\,\omega/c$. The wave reflects at the bottom plate and then propagates towards the top plate

$$\mathbf{E}_2(x,y,z) \;=\; -E_0\,\mathbf{n}_y\,\exp[ikx\cos\theta + ikz\sin\theta]\;, \tag{8.29}$$

where the sign change is due to the boundary condition, that is, the total parallel $\mathbf{E}$-field has to vanish. The sum of the fields becomes

$$\mathbf{E}(x,y,z) \;=\; \mathbf{E}_1(x,y,z) + \mathbf{E}_2(x,y,z) \;=\; -2i\,E_0\,\mathbf{n}_y\,\exp[ikz\sin\theta]\sin[kx\cos\theta]\;. \tag{8.30}$$

While this field satisfies the boundary condition at the bottom surface, it does not yet at the top plate $x = d$. Requiring that $\mathbf{E}(d,y,z) = 0$ yields $\sin[kx\cos\theta] = 0$, which is fulfilled if

$$kd\cos\theta \;=\; n\pi \qquad n \in \{1,2,..\}\;, \tag{8.31}$$

which corresponds to a 'quantization' of the normal wavenumber $k_x = k\cos\theta$

$$k_{x_n} \;=\; n\frac{\pi}{d} \qquad n \in \{1,2,..\}\;. \tag{8.32}$$

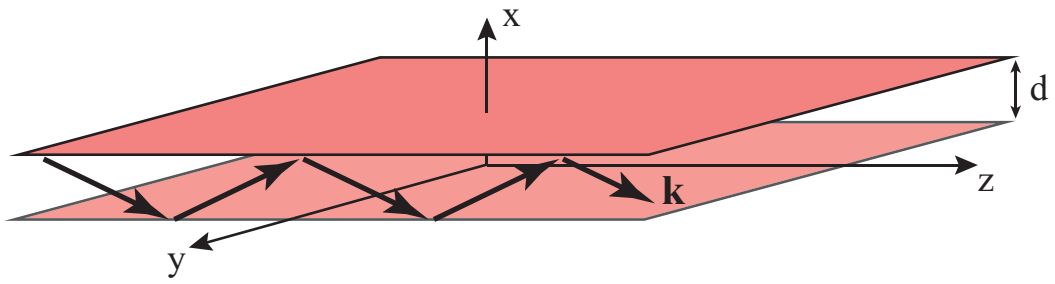

Figure 8.3: A parallel-plate waveguide with plate separation d.

Note that $n = 0$ is excluded because it yields a zero-field (trivial solution). Using $k^2 = k_z^2 + k_x^2$, we find the the propagation constant k_z of the field propagating in between of the plates in z direction is

$$k_{z_n} = \sqrt{k^2 - n^2\,[\pi/d]^2} \qquad n \in \{1, 2, ..\} \tag{8.33}$$

As long as k_{z_n} is real the field will propagate along the z direction. However, when $n\pi/d > k$ the propagation constant k_{z_n} is imaginary and the field will exponential decay in direction of z, similar to evanescent waves discussed in Section 4.4. Because $k \propto \omega$ it turns out that the waveguide acts as a high-pass filter. Frequencies below the *cut-off frequency*

$$\omega_c = \frac{n\,\pi\,c}{d\,n(\omega_c)} \qquad n \in \{1, 2, ..\} \tag{8.34}$$

cannot propagate. In summary, the solutions of the wave equation for a system of two parallel plates are characterized by a mode number n. We refer to the solutions that have no electric field in propagation direction as TE_n modes. Solutions are found only for discrete frequencies ω_n and for each mode there is a cut-off frequency below which no propagation is possible. Note, that $n(\omega_c)$ is the dispersive index of refraction of the medium between the two plates.

For propagating fields with $\omega > \omega_c$, the *phase velocity* is defined by the phase factor $\exp[ik_{z_n}z - i\omega t]$ as $v_{ph} = \omega/k_{z_n}$. On the other hand, the energy of the field and thus any information associated with it is transported at the *group velocity* $v_g = d\omega/dk_{z_n}$.

TM Modes

Let us now repeat the analysis for the case where the magnetic field is parallel to the surface of the plates. Similar to Eq. (8.28) we write

$$\mathbf{H}_1(x, y, z) = H_0\,\mathbf{n}_y\,\exp[-ikx\cos\theta + ikz\sin\theta]\;, \tag{8.35}$$

The wave reflects at the bottom plate and then propagates towards the top plate

$$\mathbf{H}_2(x, y, z) = H_0\,\mathbf{n}_y\,\exp[ikx\cos\theta + ikz\sin\theta]\;, \tag{8.36}$$

In contrast to Eq. (8.36) there is no sign change of H_0 upon reflection at the boundary. This follows from the boundary conditions (4.11) - (4.14).[1] The sum of the fields becomes

$$\mathbf{H}(x,y,z) \;=\; \mathbf{H}_1(x,y,z)+\mathbf{H}_2(x,y,z) \;=\; 2\,H_0\,\mathbf{n}_y\,\exp[ikz\sin\theta]\cos[kx\cos\theta]\;, \quad (8.37)$$

and the boundary conditions at the top interface $z = d$ lead to the condition

$$kd\cos\theta \;=\; n\pi \qquad n\in\{0,1,2\,..\}\;. \quad (8.38)$$

In contrast to the quantization condition (8.31) for TE modes, we now also find solutions for $n = 0$ ($\cos(0) \neq 0$). Thus,

$$k_{z_n} \;=\; \sqrt{k^2-n^2\,[\pi/d]^2} \qquad n\in\{0,1,..\} \quad (8.39)$$

The fundamental mode TM_0 has no cut-off frequency whereas all higher order TM do have a cut-off, similar to TE modes discussed above. The absence of a cut-off

[1] The electric field associated with $\mathbf{H}_1$ is $\mathbf{E}_1 \sim E_0[\sin\theta, 0, \cos\theta]^T$, which upon reflection becomes $\mathbf{E}_2 \sim E_0[\sin\theta, 0, -\cos\theta]^T$ because the parallel $\mathbf{E}$-field at the boundary has to vanish. Consequently, H_0 remains unchanged upon reflection.

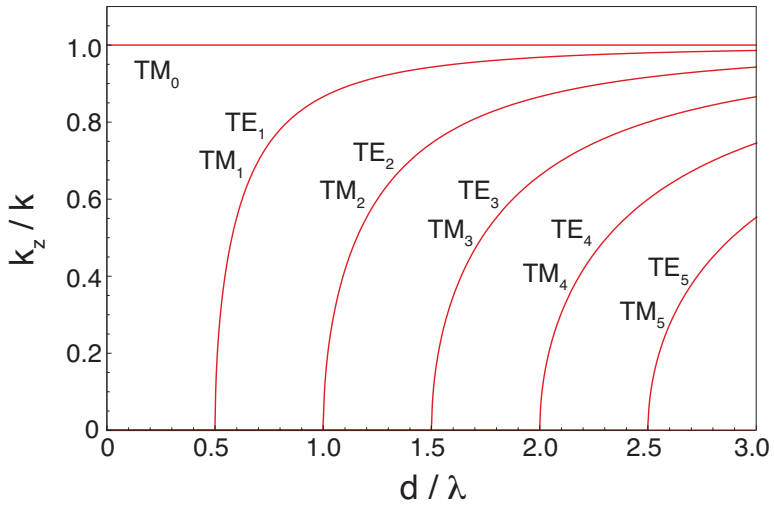

Figure 8.4: Mode structure of a parallel-plate waveguide with plate separation d. The vertical axis shows the real part of the normalized propagation constant. All modes, with the exception of TM_0 run into cut-off as the wavelength λ is increased or the plate separation d is decreased.

for the TM mode is a finding that is not restricted to two parallel plates, but holds for any waveguide made of two electrically isolated metal electrodes. For example, a coaxial cable has no cut-off, but a hollow metal waveguide (a pipe) does have a cut-off.

8.2.2 Hollow Metal Waveguides

We now confine the lateral extent of the waveguide modes. The parallel-plate waveguide then turns into a hollow metal waveguide as illustrated in Fig. 8.5. To solve for the fields in such a waveguide structure we write

$$\mathbf{E}(x,y,z) \;=\; \mathbf{E}^{xy}(x,y)\,\mathrm{e}^{-ik_z z}\;. \tag{8.40}$$

Inserting into the the Helmholtz equation (3.15) leads to

$$\left[\nabla_t^2 + k_t^2\right]\mathbf{E}^{xy}(x,y) \;=\; 0\;, \tag{8.41}$$

where $\nabla_t^2 = \partial^2/\partial x^2 + \partial^2/\partial y^2$ is the transverse Laplacian and and $k_t = [k_x^2 + k_y^2]^{1/2} = [k^2 - k_z^2]^{1/2}$ is the transverse wavenumber.

Next, we write the electric field in terms of a transverse vector in the (x,y) plane and a longitudinal vector that points along the z axis, that is,

$$\mathbf{E} \;=\; \mathbf{E}_t + \mathbf{E}_z\;. \tag{8.42}$$

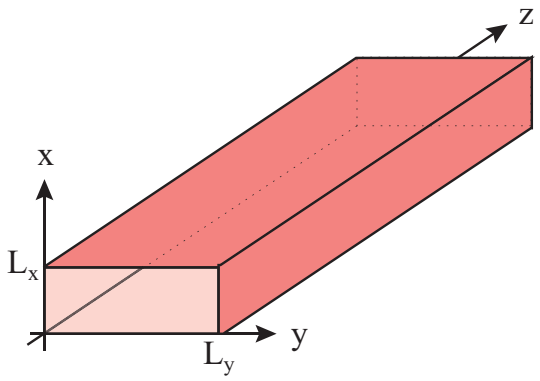

Figure 8.5: A rectangular hollow metal waveguide.

Here, $\mathbf{E}_t = \mathbf{E} \times \mathbf{n}_z$ and $\mathbf{E}_z = (\mathbf{E} \cdot \mathbf{n}_z)\mathbf{n}_z$. A similar expression can be written for the magnetic field $\mathbf{H}$. Inserting both expressions into Maxwell's equations (2.31) - (2.34), and assuming that the waveguide materials is linear and source-free, we find

$$E_x^{xy} = -Z \frac{ik}{k_t^2}\frac{\partial H_z^{xy}}{\partial y} + \frac{ik_z}{k_t^2}\frac{\partial E_z^{xy}}{\partial x} \tag{8.43}$$

$$E_y^{xy} = Z \frac{ik}{k_t^2}\frac{\partial H_z^{xy}}{\partial x} + \frac{ik_z}{k_t^2}\frac{\partial E_z^{xy}}{\partial y} \tag{8.44}$$

$$H_x^{xy} = Z^{-1}\frac{ik}{k_t^2}\frac{\partial E_z^{xy}}{\partial y} + \frac{ik_z}{k_t^2}\frac{\partial H_z^{xy}}{\partial x} \tag{8.45}$$

$$H_y^{xy} = -Z^{-1}\frac{ik}{k_t^2}\frac{\partial E_z^{xy}}{\partial x} + \frac{ik_z}{k_t^2}\frac{\partial H_z^{xy}}{\partial y}\ . \tag{8.46}$$

where Z is the wave impedance defined in Eq. (4.33). These equations show that the transverse field components E_x^{xy}, E_y^{xy} and H_x^{xy}, H_y^{xy} derive from the longitudinal field components E_z^{xy} and H_z^{xy}. Thus, it is sufficient to solve for E_z^{xy} and H_z^{xy}. So far, the discussion was general, not restricted to any particular waveguide geometry. We next discuss the particular case of a rectangular hollow metal waveguide, as illustrated in Fig. 8.5. Such waveguides are commonly used in the microwave regime, which spans the frequency range of 1-100 GHz.

TE Modes

For TE waves the field $\mathbf{E}_z^{xy}$ is zero. Thus, according to Eqs. (8.43) - (8.46) all field components can be derived from $\mathbf{H}_z^{xy}$. Following the discussion in Section 8.2.1 we find

$$\begin{aligned} H_z^{xy}(x,y) &= H_{0_z}\,\cos[k_x x]\,\cos[k_y y] \\ &= H_{0_z}\,\cos[\frac{n\pi}{L_x}x]\,\cos[\frac{m\pi}{L_y}y] \qquad n,m \in \{0,1,2..\}\ , \end{aligned} \tag{8.47}$$

with the transverse wavenumber given by

$$k_t^2 = [k_x^2 + k_y^2] = \left[\frac{n^2\pi^2}{L_x^2} + \frac{m^2\pi^2}{L_y^2}\right] \qquad n,m \in \{0,1,2..\}\ , \tag{8.48}$$

similar to the mode structure of a resonator (Eq. 8.11). Accordingly, the frequencies of the TE_{nm} modes are

$$\omega_{nm} \;=\; \frac{\pi\, c}{n(\omega_{nm})}\sqrt{\frac{n^2}{L_x^2}+\frac{m^2}{L_y^2}} \qquad n,m\in\{0,1,2,..\} \tag{8.49}$$

with $n(\omega_{nm})$ being the index of refraction. It turns out that n and m cannot both be zero because the TE_{00} does not exist. Thus, the lowest frequency mode is the TE_{01} or the TE_{10} mode. While the modes of a parallel-plate waveguide are formed by the superposition of two plane waves, the fields of a hollow rectangular waveguide follow from the superposition of four plane waves. Note that the condition of a magnetic field parallel to the waveguide surfaces leads here to TE modes, whereas in the case of two parallel plates it leads to TM modes.

The propagation constant (longitudinal wavenumber) is calculated as

$$k_z=\sqrt{k^2-k_t^2} \;=\; \sqrt{\frac{\omega_{nm}^2}{c^2}\,n^2(\omega_{nm})-\left[\frac{n^2\pi^2}{L_x^2}+\frac{m^2\pi^2}{L_y^2}\right]} \qquad n,m\in\{0,1,2\,..\}\,. \tag{8.50}$$

Since n, m cannot both be zero we find that all modes run into cut-off for low enough frequencies ω. The lowest-order mode is generally referred to as the fundamental mode or the dominant mode.

Let us choose $L_x > L_y$. In this case, the fundamental mode is the TE_{01} mode for which, according to Eqs. (8.43) - (8.46), the fields are determined as

$$\begin{aligned}
H_z^{xy} &= H_{0_z}\cos[\frac{\pi}{L_y}y] && (8.51)\\
H_y^{xy} &= i(k_z/k_t^2)\,H_{0_z}\,(\pi/L_y)\sin[\frac{\pi}{L_y}y] && (8.52)\\
E_x^{xy} &= -(ikZ/k_t^2)\,H_{0_z}\,(\pi/L_y)\sin[\frac{\pi}{L_y}y] && (8.53)\\
H_x^{xy} &= E_y^{xy} \;=\; E_z^{xy} \;=\; 0\,.
\end{aligned}$$

According to Eq. (8.40), the total fields $\mathbf{E}$ and $\mathbf{H}$ are obtained by multiplying with $\exp[-ik_z z]$. The fields of the TE_{01} mode are illustrated in Fig. 8.6.

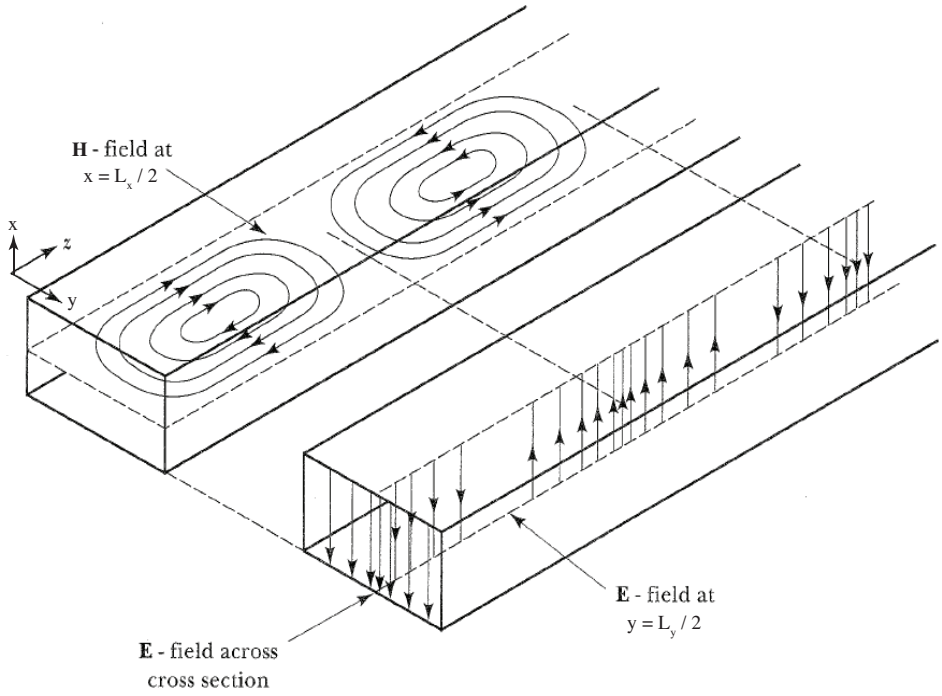

Figure 8.6: Fields of the fundamental TE_{01} mode. Adapted from *Heald & Marion, Classical Electromagnetic Radiation, Saunders College Publishing, 3rd ed. 1995.*

TM Modes

Following the discussion in Section 8.2.1, the electric field of a TM mode is

$$E_z^{xy}(x,y) \;=\; E_{0_z}\,\sin[\frac{n\pi}{L_x}x]\,\sin[\frac{m\pi}{L_y}y] \qquad n,m \in \{1,2\,..\}\,. \tag{8.54}$$

Mode indices $n = 0$ and $m = 0$ are forbidden because they lead to a zero-field solution. Thus, the lowest-order TM mode is the TM_{11} mode.

8.2.3 Optical Waveguides

Because of absorption, metal waveguides become lossy at very hight frequencies. Therefore, at optical frequencies ($200 - 800$ THz) it is more favorable to guide electromagnetic radiation in dielectric structures. The waveguiding principle is based on total internal reflection (TIR) between dielectric interfaces (see Section 4.4). In order for a wave to be totally reflected at a boundary between two dielectrics with

refractive indices n_1 and n_2 it must be incident from the optically denser medium ($n_1 > n_2$) and propagate at an angle larger than the critical angle $\theta_c = \arctan[n_2/n_1]$ measured from the surface normal. In contrast to metal waveguides, TIR in dielectric waveguides leads to evanescent fields that stretch out into the surrounding medium with the lower index of refraction n_2 (see Fig. 8.7). Thus, the boundary conditions at the interfaces become more complex.

Optical fibers are axially symmetric, that is, they consist of a dielectric rod of index n_1 (the core) surrounded by a medium of index n_2 (the cladding). For claddings of sufficient thickness the evanescent waves are strongly attenuated at the outer boundaries and it is reasonable to approximate the cladding radius as being infinite. The fields of an optical waveguide with circular cross section are described by cylindrical Bessel functions J_n of order n. To keep things simple, we will not analyze optical fibers with circular cross-sections. Instead, we focus on the dielectric slab waveguide that consists of a dielectric layer with index n_1 sandwiched between two infinite dielectrics of index $n_2 < n_1$. The mode structure is different but the physical principles are the same.

The waveguide fields have to satisfy the Helmholtz equation (3.15). Similar to Section 8.2.1 we will separate the fields into transverse electric (TE) and transverse magnetic (TM) solutions. In the former case the electric field has no vector component along the waveguide axis z, whereas in the latter case the same holds for the magnetic field. As illustrated in Fig. 8.7, a waveguide mode can be de-

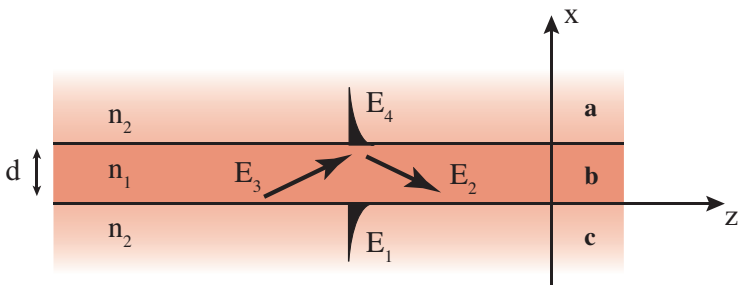

Figure 8.7: Optical step-index waveguide made of a dielectric with refractive index n_1 surrounded by a dielectric with lower index of refraction n_2. Waveguiding originates from a sequence of total internal reflections.

scribed by the superposition of four waves, namely two plane waves inside the waveguide ($0 < x < d$), an evanescent wave in the medium above the waveguide ($x > d$) and an evanescent wave below the waveguide ($x < 0$). The evanescent waves above and below the waveguide ensure that no energy is radiated away from the waveguide. Thus, the total field $\mathbf{E}$ is written in terms of partial fields $\mathbf{E}_1 .. \mathbf{E}_4$ as

$$\mathbf{E}(\mathbf{r}) = \begin{cases} \mathbf{E}_1(\mathbf{r}) & x < 0 \\ \mathbf{E}_2(\mathbf{r}) + \mathbf{E}_2(\mathbf{r}) & 0 < x < d \\ \mathbf{E}_4(\mathbf{r}) & x > d \end{cases} \tag{8.55}$$

In the following we will discuss the TM and TE cases separately.

TM Modes

Denoting the $\mathbf{k}$ vector in the waveguide (medium 1) as $\mathbf{k}_1 = [k_{x_1}, 0, k_z]$ and outside the waveguide (medium 2) as $\mathbf{k}_2 = [k_{x_2}, 0, k_z]$, the partial fields of a TM mode are calculated as follows

$$\mathbf{E}_1 = E_1 \begin{pmatrix} k_z/k_2 \\ 0 \\ k_{x_2}/k_2 \end{pmatrix} \mathrm{e}^{-ik_{x_2}x + ik_z z}, \quad \mathbf{H}_1 = \frac{E_1}{Z_2} \begin{pmatrix} 0 \\ 1 \\ 0 \end{pmatrix} \mathrm{e}^{-ik_{x_2}x + ik_z z} \tag{8.56}$$

$$\mathbf{E}_2 = E_2 \begin{pmatrix} k_z/k_1 \\ 0 \\ k_{x_1}/k_1 \end{pmatrix} \mathrm{e}^{-ik_{x_1}x + ik_z z}, \quad \mathbf{H}_2 = \frac{E_2}{Z_1} \begin{pmatrix} 0 \\ 1 \\ 0 \end{pmatrix} \mathrm{e}^{-ik_{x_1}x + ik_z z} \tag{8.57}$$

$$\mathbf{E}_3 = E_3 \begin{pmatrix} k_z/k_1 \\ 0 \\ -k_{x_1}/k_1 \end{pmatrix} \mathrm{e}^{ik_{x_1}x + ik_z z}, \quad \mathbf{H}_3 = \frac{E_3}{Z_1} \begin{pmatrix} 0 \\ 1 \\ 0 \end{pmatrix} \mathrm{e}^{ik_{x_1}x + ik_z z} \tag{8.58}$$

$$\mathbf{E}_4 = E_4 \begin{pmatrix} k_z/k_2 \\ 0 \\ -k_{x_2}/k_2 \end{pmatrix} \mathrm{e}^{ik_{x_2}x + ik_z z}, \quad \mathbf{H}_4 = \frac{E_4}{Z_2} \begin{pmatrix} 0 \\ 1 \\ 0 \end{pmatrix} \mathrm{e}^{ik_{x_2}x + ik_z z} \tag{8.59}$$

Here we used the continuity of k_z and the transversality of the fields ($\nabla \cdot \mathbf{E} = i\mathbf{k} \cdot \mathbf{E} = 0$). To calculate the magnetic field we used Maxwell's curl equation (2.32) and assumed linear material equations (3.7). Note that in order for the fields to be evanescent outside the waveguide we require $k_z > k_2$. On the other hand, for the

fields to be propagating inside the waveguide we require $k_z < k_2$. Thus, waveguide modes will exist only in the interval $k_2 < k_z < k_1$.

Having defined the partial fields we know have to match them at the boundaries $x = 0$ and $x = d$. The continuity of the parallel components of electric and magnetic fields lead to

$$\begin{bmatrix} k_{x_2}/k_2 & -k_{x_1}/k_1 & k_{x_1}/k_1 & 0 \\ 1/Z_2 & -1/Z_1 & -1/Z_1 & 0 \\ 0 & k_{x_1}/k_1 \exp[-ik_{x_1}d] & -k_{x_1}/k_1 \exp[ik_{x_1}d] & k_{x_2}/k_2 \exp[ik_{x_2}d] \\ 0 & 1/Z_1 \exp[-ik_{x_1}d] & 1/Z_1 \exp[ik_{x_1}d] & -1/Z_2 \exp[ik_{x_2}d] \end{bmatrix} \begin{bmatrix} E_1 \\ E_2 \\ E_3 \\ E_4 \end{bmatrix} = 0 \tag{8.60}$$

This is a homogeneous system of linear equations, that is, an eigenvalue problem. The reason why we end up with a *homogeneous* system of equations is the absence of an excitation, which means that there are no sources or incident fields. Thus, we are looking for solutions that the system supports in absence of an external driving force, similar to an undriven harmonic oscillator. A homogeneous system of equations has solutions only if the determinant of the matrix acting on the eigenvector $[E_1, E_2, E_3, E_4]^T$ vanishes, that is,

$$\begin{vmatrix} k_{x_2}/k_2 & -k_{x_1}/k_1 & k_{x_1}/k_1 & 0 \\ 1/Z_2 & -1/Z_1 & -1/Z_1 & 0 \\ 0 & k_{x_1}/k_1 \exp[-ik_{x_1}d] & -k_{x_1}/k_1 \exp[ik_{x_1}d] & k_{x_2}/k_2 \exp[ik_{x_2}d] \\ 0 & 1/Z_1 \exp[-ik_{x_1}d] & 1/Z_1 \exp[ik_{x_1}d] & -1/Z_2 \exp[ik_{x_2}d] \end{vmatrix} = 0 \tag{8.61}$$

Writing out the expression for the determinant and arranging terms we obtain

$$1 + \frac{(Z_2 k_{x_2}/k_2 - Z_1 k_{x_1}/k_1)}{(Z_2 k_{x_2}/k_2 + Z_1 k_{x_1}/k_1)} \frac{(Z_1\, k_{x_1}/k_1 - Z_2 k_{x_2}/k_2)}{(Z_1 k_{x_1}/k_1 + Z_2 k_{x_2}/k_2)} \exp[2ik_{x_1}d] = 0\,, \tag{8.62}$$

which can be written in the form

$$1 + r^p_{ab}(k_z)\, r^p_{bc}(k_z)\, \mathrm{e}^{2ik_{x_1}d} = 0 \tag{8.63}$$

Here, r^p_{ab} and r^p_{bc} are the Fresnel reflection coefficients for p polarization, as defined in Eq. (4.39). The subscript 'ab' indicates that the reflection is measured between the upper medium (medium a in Fig. 8.7) and the waveguide (medium b in Fig. 8.7). Similarly, the subscript 'bc' is the reflection coefficient measured

between the waveguide and the lower medium (medium 3 in Fig. 8.7). Note that

$$k_{x_1} = \sqrt{k_1^2 - k_z^2} = \sqrt{\frac{\omega^2}{c^2}\mu_1\varepsilon_1 - k_z^2}, \quad k_{x_2} = \sqrt{k_2^2 - k_z^2} = \sqrt{\frac{\omega^2}{c^2}\mu_2\varepsilon_2 - k_z^2}\,, \tag{8.64}$$

and hence Eq. (8.63) defines the characteristic equation for the eigenvalues k_z. Every solution for k_z defines a waveguide mode. It has to be emphasized that the sign of the square roots in the expressions for k_{x_1} and k_{x_2} has to be chosen such that the imaginary part is positive. This ensures that the fields decay exponentially with distance from the waveguide (evanescent fields). The other sign would imply an exponential increase, which would violate energy conservation.

TE Modes

A similar analysis can be applied for TE polarized fields, for which the electric field is parallel to the boundaries. The resulting characteristic equation for k_z is

$$1 \;+\; r^s_{ab}(k_z)\, r^s_{bc}(k_z)\, \mathrm{e}^{2ik_{x_1}d} \;=\; 0 \tag{8.65}$$

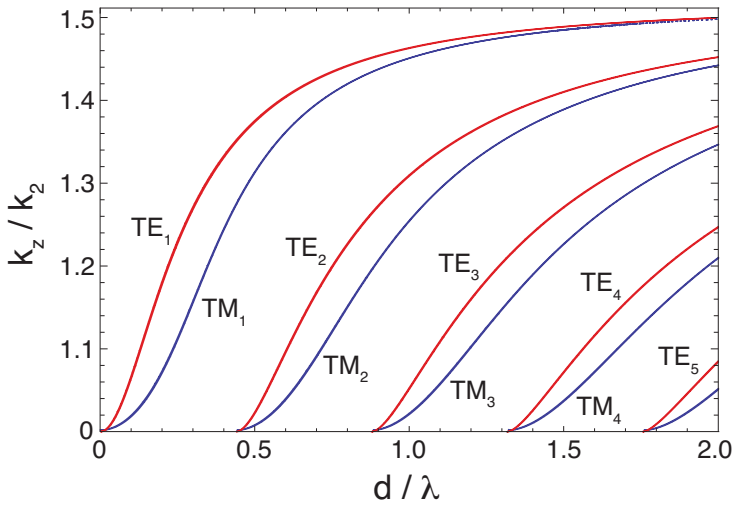

Figure 8.8: Mode structure of a dielectric slab waveguide with $n_1 = 1.5$ (glass) and $n_2 = 1$ (air). The vertical axis shows the real part of the normalized propagation constant k_z. There is no cut-off for the fundamental modes TM_1 and TE_1.

with r_{ab}^p and r_{bc}^p being the Fresnel reflection coefficients for s polarization.

As shown in Fig. 8.8, the mode structure for the dielectric waveguide is similar to the mode structure of a parallel-plate waveguide in Fig. 8.4. However, due to the different Fresnel reflection coefficients for TE and TM modes, the curves for TM and TE modes are no longer the same and split into separate curves. The fundamental modes TE_1 and TM_1 have no cut-off and in the limit $d/\lambda \to 0$ they become plane waves ($k_z = k_2$). Similarly, in the limit $d/\lambda \to \infty$ the modes become plane waves propagating in the higher dielectric ($k_z = k_1$).

8.2.4 Optical Fibers

In many regards the mode structure in optical fibers is similar to the mode structure of a dielectric slab waveguide. There are, however, also some relevant differences. First, an optical fiber is a waveguide that confines the electromagnetic field in two dimensions which, according to Section 8.2.2, leads to two mode indices nm. One of them specifies the angular dependence of the fields [$\sin m\phi$, $\cos m\phi$] and the other one the radial dependence [$J_n(\rho)$, $H_n^{(1)}(\rho)$]. Second, besides pure TE and

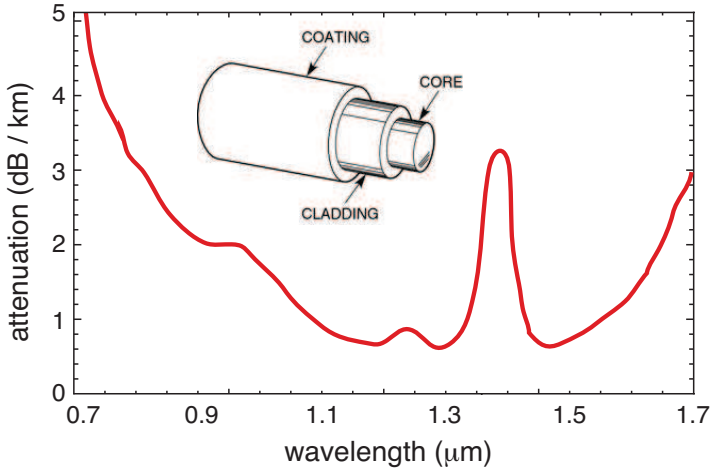

Figure 8.9: Attenuation in an optical fiber. Lowest propagation losses are obtained at wavelengths of $\sim 1.3\,\mu$m and $\sim 1.5\,\mu$m.

TM modes there are also hybrid modes, which are classified as HE and EH modes. HE modes have TE flavor whereas the EH modes have more TM character.

There are two basic versions of optical fibers: gradient index fibers and step-index fibers. The former has an index of refraction profile that varies gradually with radius [$n = n(\rho)$], whereas the latter exhibits an abrupt transitions between two refractive indices, similar to the slab waveguide. Step-index fibers are the most commonly used fibers and usually the index difference is very small, that is $(n_1 - n_2)/n_1 \ll 1$, which is referred to as the *weakly guiding* condition. Polarized weakly guided modes are denoted as LP_{nm} modes. A single-mode fiber supports only the fundamental LP_{01} mode and all higher-order modes are suppressed by the cut-off condition. Fig. 8.9 shows the propagation loss in a modern optical fiber. The losses on the short-wavelength side are due to Rayleigh scattering and the losses at the long wavelength end are due to infrared absorption. The bumps are absorption bands of molecular bonds, such as OH^-. The lowest attenuation is obtained near 1.3 and 1.5 μm and is the reason why fiber-optic communication is operated at these wavelengths.